JBMR Plus, 2024, **8**, ziae014
https://doi.org/10.1093/jbmrpl/ziae014
Advance access publication: February 1, 2024
Research Article

Correlation between tibial and femoral bone and cartilage changes in end-stage knee osteoarthritis

Fahimeh Azari[1], William Colyn[2,3,4], Johan Bellemans[3,5], Lennart Scheys[6], G.H. van Lenthe[1,*]

[1]Biomechanics Section, Mechanical Engineering, KU Leuven, Leuven, Belgium
[2]Department of Orthopedic Surgery, AZ Turnhout, Turnhout, Belgium
[3]Faculty of Medicine and Life Sciences, Hasselt University, Diepenbeek, Belgium
[4]Limburg Clinical Research Center, ZOL Genk, Genk, Belgium
[5]GRIT Belgian Sports Clinic, Leuven, Belgium
[6]Department of Orthopaedics, University Hospitals Leuven, Leuven, Belgium
*Corresponding author: G. Harry van Lenthe, PhD, Biomechanics Section, KU Leuven, Celestijnenlaan 300C, 3001 Leuven, Belgium (harry.vanlenthe@kuleuven.be).

Abstract

Knee osteoarthritis is a whole joint disease highlighting the coupling of cartilage and bone adaptations. However, the structural properties of the subchondral bone plate (SBP) and underlying subchondral trabecular bone (STB) in the femoral compartment have received less attention compared to the tibial side. Furthermore, how the properties in the femoral compartment relate to those in the corresponding tibial site is unknown. Therefore, this study aimed to quantify the structural bone and cartilage morphology in the femoral compartment and investigate its association with those of the tibial plateau. Specifically, tibial plateaus and femoral condyles were retrieved from 28 patients with end-stage knee-osteoarthritis (OA) and varus deformity. The medial condyle of tibial plateaus and the distal part of the medial femoral condyles were micro-CT scanned (20.1 μm/voxel). Cartilage thickness (Cart.Th), SBP, and STB microarchitecture were quantified. Significant ($P < <.001$; $0.79 \leq r \leq 0.97$) correlations with a relative difference within 10% were found between the medial side of the femoral and tibial compartments. The highest correlations were found for SBP porosity ($r = 0.97$, mean absolute difference of 0.50%, and mean relative difference of 9.41%) and Cart.Th ($r = 0.96$, mean absolute difference of 0.18 mm, and relative difference of 7.08%). The lowest correlation was found for trabecular thickness ($r = 0.79$, mean absolute difference of 21.07 μm, and mean relative difference of 5.17%) and trabecular number ($r = 0.79$, mean absolute difference of 0.18 mm^{-1}, and relative difference of 5.02%). These findings suggest that the distal femur is affected by OA in a similar way as the proximal tibia. Given that bone adaptation is a response to local mechanical forces, our results suggest that varus deformity similarly affects the stress distribution of the medial tibial plateau and the medial distal femur.

Keywords: tibiofemoral, osteoarthritis, subchondral bone, tibial plateau, varus alignment, cartilage morphology

Lay Summary

Knee osteoarthritis is a disease that affects the knee joint. In knee osteoarthritis, the cartilage in the knee joint gradually wears away over time, and the bone experiences changes in its microstructure. As a result, the bones in the joint may rub against each other, causing pain, stiffness, and reduced mobility. Thus far, most attention has focused on the lower leg bone (tibia), whereas less is known on the upper leg bone (femur). To bridge the knowledge gap, we quantified cartilage thickness (Cart.Th) and bone structure in the femur and tibia of 28 bow-legged persons who suffered from advanced knee osteoarthritis. Using detailed scans, we measured the thickness of the cartilage and the microstructure of the bones. We found that Cart.Th was strikingly similar in the femur and in the tibia; bone microstructure was very similar, too. In summary, our findings suggest that knee osteoarthritis affects the femur in a similar way as the tibia. This similarity might be because the knee joint adjusts to the local mechanical loading it experiences. These data hold potential in assisting doctors to devise more effective strategies for alleviating knee discomfort and enhancing overall knee health.

Received: November 30, 2023. **Accepted:** February 1, 2024

Graphical Abstract

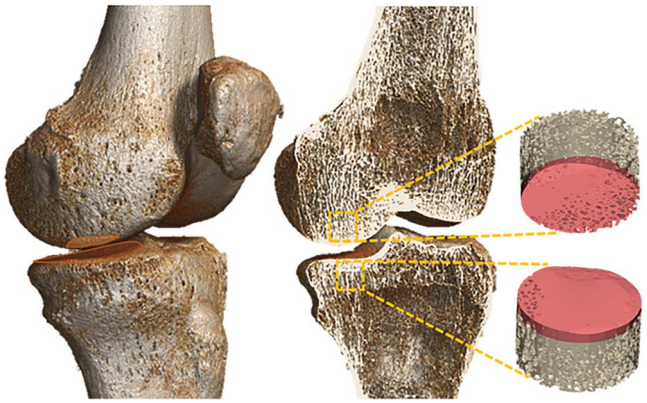

Introduction

Osteoarthritis (OA) is a common and progressive joint disease. OA is most common in the knee and affects 83% of patients suffering from OA.[1] The high prevalence and multimorbidity demonstrate the significant burden of knee OA. Although OA was previously considered a primary disorder of articular cartilage, recent studies suggest that OA influences the whole joint and highlight the crucial contribution of subchondral bone in OA development and its interaction with articular cartilage.[2,3] Knee OA involves both the proximal tibia and distal femur. In varus OA knees, the medial tibiofemoral compartment of the knee joint is more damaged than the lateral compartment.[4,5] This is likely related to the larger mechanical loading that the medial compartment bears, which amounts for 60%–80% of the total compressive forces transferred across the knee.[6] With increasing varus deformity, the load-bearing axis is shifting further away from a central knee position toward the medial side, which even further pronounces this uneven load distribution.[7] Indeed, varus deformity results in a significantly higher subchondral bone volume fraction (BV/TV) in the medial compartment, whereas valgus alignment results in a significantly higher subchondral BV/TV in the lateral compartment.[3,8-10] Furthermore, an increase in varus angle correlates with more sclerosis in the medial compartment.[3,9-11]

It is well-known that knee OA involves the proximal tibia and distal femur. Yet, little is known about the specific changes in bone microstructure that occur at both sides. Using magnetic resonance imaging in vivo, Beuf et al.[12] measured approximately 4 cm of the proximal tibia and 4 cm of the distal femur. For the trabecular bone in these volumes, BV/TV, trabecular number (Tb.N), and thickness of the trabeculae (Tb.Th) were higher in the femur than in the tibia, while trabecular separation (Tb.Sp) was lower. They also reported that with advancing OA the differences between femur and tibia disappeared except for a small remaining difference in BV/TV. Using micro-CT on bone biopsies taken from the medical and lateral condyles of the proximal tibia and distal femur, Lahm et al.[13] also identified regional differences during the osteoarthritic process and reported that BV/TV in the femur was higher than in the tibia. They also showed that the medial condyles in the femur and tibia showed the most pronounced changes in BV/TV and Tb.N. In contrast to the study of Beuf et al.,[12] the difference became larger with advancing OA.

Hence, the inconsistent outcomes in prior studies regarding the association between tibial and femoral adaptations in knee OA underscore the necessity of exploring the interdependence of altered tibial properties with those of the femur. Furthermore, only limited data have been reported on the microstructural properties at the femoral side like cartilage thickness (Cart.Th), thickness of the subchondral bone plate (SBP), and microstructural properties of the underlying subchondral trabecular bone (STB).

This study represents a follow-up to our previous investigation, where we examined region-specific microstructural adaptations of the subchondral bone in tibial plateaus concerning the mechanical axis deviation (MAD).[11] As demonstrated in our prior research[11] and supported by existing literature,[2,3] it has been established that the lateral side of the tibial plateau in end-stage varus OA is less affected. Therefore, in the current study, we aimed to visualize and quantify cartilage and bone microstructure in the medial tibial plateau and medial distal femur in end-stage varus knee OA. We focused exclusively on the anterior medial tibial plateau, as it was identified in our previous work[11] as the most affected region and the corresponding femoral region.

Materials and methods

Specimens

Approval for this study was granted by the ZOL Genk ethical committee (approval number of the project: B371201939696). Forty-nine entire tibial plateaus and the distal medial femoral condyles were retrieved from patients with varus knee alignment and suffering from end-stage knee OA (Kellgren-Lawrence Grade[14] equal to 3 or 4) who underwent total knee arthroplasty. Twenty-one specimens were excluded because the thickness of the STB layer in the medial tibial plateau was less than 3 mm, which does not allow for reliable measurement of bone microstructure.[15-17] This study used 18 tibial plateau specimens that were obtained from a previous study.[11] A detailed summary of patients' characteristics for the 28 specimens (11 males, 17 females, 15 right and 13 left knees) is given in Table 1. The specimens were rinsed and placed in a plastic bag for preservation in a freezer at −20°C.

Table 1. Summary of patient characteristics.

Parameters	End-stage varus knee osteoarthritis, $n = 28$
Age	69.6 yr ± 6.6 yr
BMI	31.4 kg/m^2 ± 4.5 kg/m^2
[a]KL Grade	3.3 ± 0.6

Data represent mean values ± SD. Abbreviation: [a]KL grade, Kellgren-Lawrence grade.

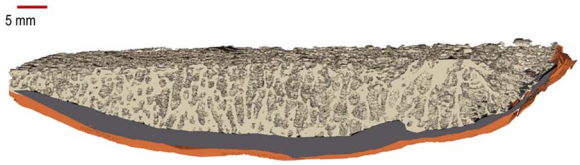

Figure 1. A representative model of the segmented distal medial femoral condyle of coronal micro-CT cross-sections. The bottom layer represents the segmented cartilage, the middle layer represents the segmented SBP, and the top layer represents the segmented STB.

Mechanical joint alignment

As part of standard clinical practice, full-leg radiographs were acquired with the patellae oriented forward.[18] Following this, W.C. conducted a series of radiographic measurements using the AGFA PACS software package (AGFA MIMOSA VIPS 1.3.00). The femoral mechanical axis was determined as the line connecting the center of the femoral head to the center of the knee, while the tibial mechanical axis was defined as the line connecting the center of the knee to the center of the ankle. Three alignment parameters were measured in this study. First, the hip–knee–ankle angle (HKA) was calculated as the angle between the mechanical axes of the femur and tibia, as assessed on a full-length lower limb radiograph.[18] The HKA angle represented the deviation from 180°, with negative values indicating varus alignment and positive values indicating valgus alignment. Second, the MAD was defined as the distance between the mechanical axis line and the center of the knee. Lastly, the medial proximal tibial angle (MPTA) was defined as the angle formed between the tibial mechanical axis and the knee joint line of the proximal tibia. The knee joint line of the proximal tibia is a line connecting the proximal ends of the medial and lateral edges of the tibial plateau.[19]

Subchondral bone microarchitecture

Micro-CT imaging

Micro-CT scans were conducted using a desktop micro-CT scanner (Skyscan 1272, Bruker). The tibial plateaus specimens were divided into a medial and lateral condylar section through the eminentia tibiae. The distal part of the medial femoral condyle and the medial condyle of the tibial plateau were wrapped in plastic film and fixed in the sample holder using mounting foam to minimize motion artifacts during the scanning. The micro-CT scans were performed with 100 kVp source voltage, 100 mA current, 0.4° rotation step, 180° rotation, 735 ms exposure time, and an averaging of 4 frames. Additionally, a 0.5 mm-thick aluminum and 0.038 mm-thick copper filter were utilized to reduce beam hardening artifacts.

Subsequently, the projection images were reconstructed into 20.1 μm isotropic voxel size using filtered back-projection algorithm (NRecon software; v1.7.5.2, Skyscan-Bruker). The reconstructed images were saved as 8-bit images with 256 gray levels, where a bmp value of 0 represented air and 255 represented mineralized tissue. Prior to reconstruction, the NRecon software's CS rotation option was employed to align the image stack's z-axis with the anatomical superior–inferior axis of each plateau, based on visual inspection of the tibial cut.

Image segmentation

Noise in the images was reduced using a 3D median filter ($\sigma = 2$). The images were then binarized using fixed global thresholding (87 gray value), and further noise reduction was performed using the despeckler function (CTAn software; 1.19.4.0, Skyscan-Bruker). Following this, the medial condyle of the distal femur and the medial tibial plateau were both divided into 3 sub-regions, including cartilage, SBP, and STB, as detailed below.

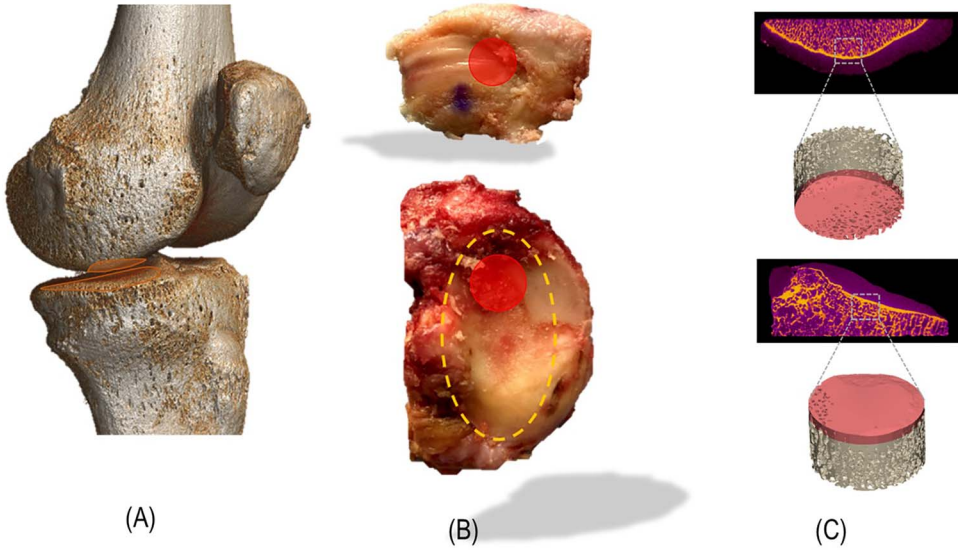

Figure 2. 3D rendering of the entire knee (A). Location of the VOIs on the photograph of an excised distal medial femoral condyle from a right knee (B, top), and on the medial condyle of the tibial plateau, the dash-lined ellipse shows the load-bearing region (B, bottom); the filled circle is the investigated VOI. 3D rendering of the VOI on the coronal grey-scale image of medial femoral condyle (C, top) and medial tibial plateau (C, bottom), including SBP and STB.

Table 2. Summary of mechanical joint alignment characteristics.

Parameters	End-stage varus knee osteoarthritis, $n = 28$
MAD	30.5 mm ± 12.6 mm [14–69.7 mm]
HKA	8.7° ± 3.7° [3.9–22°]
MPTA	86.3° ± 2.6° [78.2–90.2°]

Data represent means ± SD [minimum–maximum]. Abbreviations: HKA, hip–knee–ankle angle; MAD, mechanical axis deviation; MPTA, mechanical proximal tibial angle.

Cartilage segmentation

A semi-automatic segmentation method[3] was implemented to segment cartilage. More specifically, bone and marrow were first excluded by applying a negative mask (image minus the "bone and marrow" mask). Then, cartilage was segmented by thresholding (CTAn software).

SBP segmentation from underlying STB

SBP was separated from the underlying STB in the coronal images.[2,3] Thereto, SBP boundaries were manually contoured every 10th coronal slice (0.20 mm) and subsequently interpolated for the images in between (CTAn software). A representative model of a fully segmented distal medial femoral condyle of coronal micro-CT cross-sections is shown in Figure 1.

Volume of interests definition

In the axial image dataset of the medial tibial plateau, the largest possible elliptical ROI was indicated within the inner condylar boundary of the medial tibial plateau to indicate the load-bearing region.[20-22] A cylindrical volume of interests (VOIs) was located at the center of the anterior half of the ellipse; this is the region where most bone adaptation occurs.[11] For the femoral condyle, a cylindrical VOI was defined in the middle of distal part of the medial condyle (Figure 2). The femoral distal cut did not allow for the definition of multiple VOIs with a 10 mm diameter because, to satisfy the continuum assumption, it was necessary to define the VOI with a minimum thickness of 3 mm. This requirement could only be met in the middle of the distal part of the medial condyle. Each cylindrical VOI measured 10 mm in diameter and included, depending on the specimen, an STB layer of 3–5 mm, as measured from the inferior border of the SBP, to satisfy the continuum assumption for trabecular bone.[15,16]

Morphometric analysis

All morphometric parameters were quantified using CTAn software. Cart.Th (mm), average 3D Tb.Th (μm), Tb.Sp (μm), Tb.N (1/mm), and structure model index (SMI) were calculated based on the sphere fitting method.[23,24] Bone volume fraction (BV/TV) was calculated as the ratio of the number of bone voxels to the total number of voxels in a given VOI. For the SBP within each VOI, SBP thickness (SBP.Th) and SBP porosity (SBP.Po) were calculated. SBP.Th (mm) was calculated using the sphere-fitting method. SBP.Po was computed as the percentage of pore volume within the total tissue volume. More specifically, the number of voxels segmented as pores within the SBP VOI was divided by the total number of SPB voxels inside the VOI.

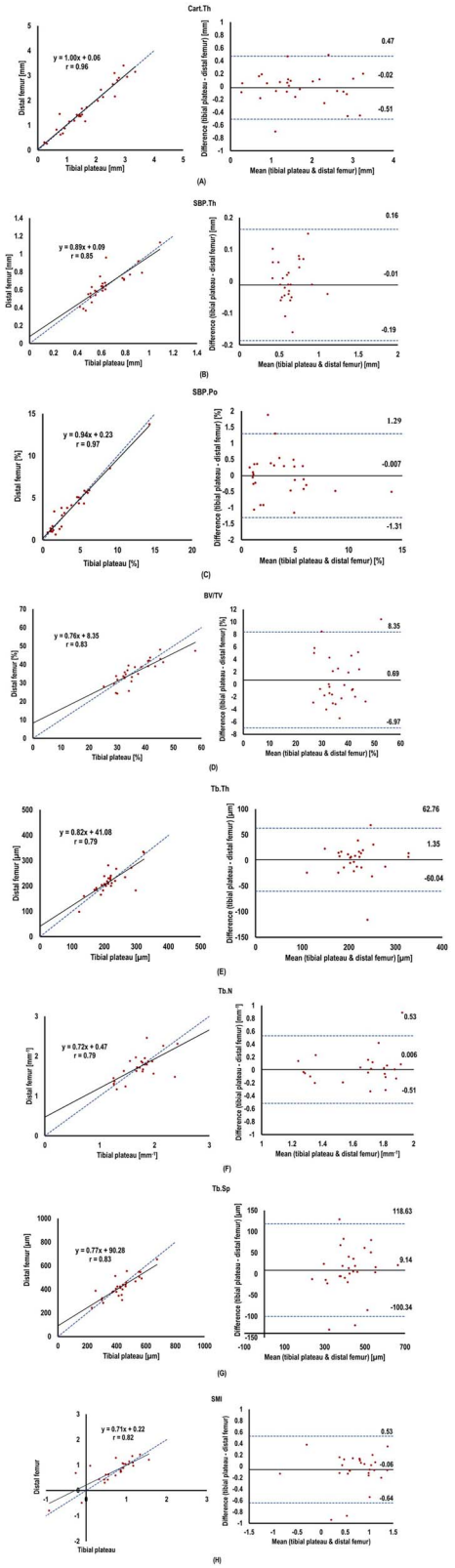

Figure 3. Scatter plots (left) and Bland–Altman (right) showing associations between Cart.Th, SBP, and STB microarchitecture parameters in the distal medial condyle of the femur and the medial tibial plateau. In the scatter plots, the dashed line represents the line y = x. In the Bland–Altman plots, the dashed lines show upper and lower confidence levels. Microarchitecture parameters include SBP.Th, SBP.Po, BV/TV, Tb.Th, Tb.N, Tb.Sp, and trabecular SMI. Panel A Title: Cart.Th. Panel B Title: SBP.Th. Panel C Title: SBP.Po. Panel D Title: BV/TV. Panel E Title: Tb.Th. Panel F Title: Tb.N. Panel G Title: Tb.Sp. Panel H Title: SMI.

Table 3. Summary of cartilage thickness (Cart.Th), subchondral bone plate (SBP), and subchondral trabecular bone (STB) microarchitecture parameters in the distal medial condyle of the femur and the medial tibial plateau, including both absolute and relative differences between the 2 sites.

Parameters	Distal femur (Mean ± SD)	Tibial plateau (Mean ± SD)	Mean absolute difference	Mean relative difference (%)	*r*
Cart.Th (mm)	1.73 ± 0.9	1.71 ± 0.8	0.18	7.08	0.96[a]
SBP.Th (mm)	0.64 ± 0.17	0.63 ± 0.16	0.06	4.97	0.85[a]
SBP.Po (%)	3.70 ± 2.97	3.69 ± 2.90	0.50	9.41	0.97[a]
BV/TV (%)	35.90 ± 6.36	36.59 ± 6.98	3.08	4.22	0.83[a]
Tb.Th (μm)	216.92 ± 47.30	218.29 ± 47.71	21.07	5.17	0.79[a]
Tb.N (1/mm)	1.76 ± 0.39	1.77 ± 0.41	0.18	5.02	0.79[a]
Tb.Sp (mm)	421.50 ± 92.44	430.64 ± 95.72	39.36	4.88	0.83[a]
SMI	0.74 ± 0.49	0.69 ± 0.50	0.20	9.85	0.82[a]

[a] $P << 0.001$ Microarchitecture parameters include SBP thickness (SBP.Th), SBP porosity (SBP.Po), BV/TV, bone volume fraction; trabecular thickness (Tb.Th), trabecular number (Tb.N), trabecular separation (Tb.Sp), and trabecular structural model index (SMI).

Statistics

Correlations between Cart.Th, SBP (SBP.Th, SBP.Po), and STB (BV/TV, Tb.Th, Tb.Sp, Tb.N, SMI) microarchitecture of the medial distal femur and the medial tibial plateau were examined using Pearson's correlation and Bland–Altman plots with corresponding absolute mean difference and 95% limits of agreement. All statistical analyses were performed using Rstudio (2021.09.1, RStudio), with significance level set to $P < .001$ following a Bonferroni correction for multiple testing.

Results

Mechanical joint alignment

The MAD, HKA, and MPTA values were calculated, confirming varus deformities for all the specimens, and are presented in Table 2.

Cartilage and bone morphometry

Scatter and Bland–Altman plots, demonstrating associations between Cart.Th, SBP, and STB microarchitecture parameters in the distal medial condyle of the femur and the medial tibial plateau are shown in Figure 3. A summary of Cart.Th, SBP, and STB microarchitecture parameters in the medial side of the femoral and tibial compartments, including both absolute and relative differences between the 2 sites, is provided (Table 3). Statistically significant associations ($P << .001$; r ranging from 0.79 up to 0.97) with relative differences within 10% were found for all microarchitectural parameters of cartilage and subchondral bone between the medial femoral condyle and the medial tibial plateau (Figure 3 and Table 3). The SBP.Po ($r = 0.97$, Figure 3C; mean relative difference = 9.41%, Table 3) and Cart.Th ($r = 0.96$, Figure 3A; mean relative difference = 7.08%, Table 3) showed the highest agreement, while the trabecular thickness ($r = 0.79$, Figure 3E; mean relative difference = 5.17%, Table 3) and Tb.N ($r = 0.79$, Figure 3F; mean relative difference = 5.02%, Table 3) showed the least agreement between the medial distal femur and the medial tibial plateau. No evidence of bias was observed in any of the Bland–Altman plots.

Discussion

In knee, OA structural changes occur in the cartilage and in the subchondral bone. Thus far, most attention has gone to the tibial plateau as the mechanical shock absorber of the knee joint[25] and little is known about changes occurring at the femoral side. In this study, we visualized and quantified Cart.Th and bone microstructure in medial femoral condyle and the medial tibial plateau in patients with end-stage OA with varus malalignment. Our major finding is that there is a strong correlation between Cart.Th and bone microarchitecture among the tibial and femoral compartments of the knee joint in the medial side ($P << .001$; r ranging from 0.79 up to 0.97). We thus demonstrate that the bone microstructure of femoral side is similar to that of tibial side in the medial condyle in end-stage OA knees. The strongest correlations were found for SBP.Po and Cart.Th ($P << .001$, $r = 0.97$ and 0.96, respectively).

Our data add to the rather limited and inconclusive data on the association between femoral and tibial bone architecture in OA knees. An earlier study demonstrated that, when comparing bone microstructure of the femoral and tibial sides in healthy, mild, and severe OA, patients with severe OA exhibited substantially lower absolute differences in mean values for all parameters.[12] We showed that, at least in end-stage OA, Cart.Th, SBP, and STB microarchitecture parameters in the distal medial femoral condyle and the medial tibial plateau are significantly correlated. We found that BV/TV in the distal medial femoral condyle was close to that of medial tibial plateau. In contrast, Lahm et al.[13] have shown a lower BV/TV for the tibia plateau than the corresponding femoral site and demonstrated that this difference increases as OA advances. Beuf et al.[12] demonstrated significant differences in the trabecular bone structure of the femur and tibia for mild OA and a control group, and these variations decreased with the progression of OA except for BV/TV. We hypothesize that these different findings are related to differences in the particular volume that was analyzed. In our analyses, the VOI was the anterior medial region of the tibia, which we had identified in a previous work as the site exhibiting the most pronounced adaptation.[11] As previous studies did not examine region-specific changes in the tibia plateau, but rather much larger volumes such as the entire medial plateau, they have reported lower BV/TV for tibial plateau than in our study.

Our study has several potential limitations. First, with 28 specimens, the sample size was limited. Although we collected a total of 49 tibial plateaus, 21 specimens were excluded because the STB layer was too small to allow for an unbiased morphological analysis. In our previous study,[11] we conducted an evaluation of potential exclusion bias and found no evidence of bias. Despite this small number

of specimens, we nevertheless found statistically significant correlations between the tibia and femur in Cart.Th and structural bone parameters. Second, our study was limited to varus cases due to their higher prevalence compared to valgus cases. However, we hypothesize that similar correlations between the lateral tibial plateau and the lateral distal femur would be observed in valgus cases as well. Thus, we could not extend our hypothesis about the correlation between the tibia and femur compartment of the tibiofemoral joint in end-stage OA for valgus cases. Furthermore, all specimens were end-stage knee OA; further studies are needed to examine the correlation between the tibia and femur in the earlier stage of OA and during OA progression. The choice of end-stage knee OA samples in our study was made to focus on the advanced pathological changes that often lead to clinical symptoms and surgical intervention. Moreover, previous studies have reported inconsistent outcomes regarding the association between tibial and femoral adaptations in knee OA, particularly in end-stage OA.[12,13] This underscores the necessity to explore the interdependence of tibial microstructures with those of the femur in end-stage OA.

Third, we examined structural changes only and did not assess mechanical properties. As the subchondral bone microarchitecture is related to knee joint loading indices in end-stage knee OA patients,[9,26] therefore, to gain a better understanding on the distribution of force across the tibia and femur this, future research should elucidate the correlation between knee compartments in the tibia and femur of OA knees in the distribution of mechanical loading.

Conclusion

In summary, in patients with end-stage knee OA, we found significant correlations between Cart.Th and structural bone parameters of the distal medial femoral condyle and the medial tibial plateau as the most affected compartments in varus knees.[11] We conclude that in end-stage knee, OA the medial femoral condyle is affected similarly as the medial condyle of the tibial plateau. These findings contribute to a better understanding of the bone changes occurring in varus OA knees.

Author contributions

Fahimeh Azari contributed to research design, acquisition, analysis, interpretation of data, and drafting the paper. William Colyn contributed to research design, acquisition, interpretation of data, and revision of the paper. Johan Bellemans contributed to research design. Lennart Scheys [share last authorship] contributed to research design, interpretation of data, and revision of the paper. G. Harry van Lenthe [share last authorship] contributed to research design, acquisition, interpretation of data, and revision of the paper. All authors have read and approved the final submitted manuscript.

Funding

This study is part of Limburg Clinical Research Center supported by Hasselt University, Ziekenhuis Oost-Limburg and Jessa Hospital and was funded in part by KU Leuven Internal Funds (C24/16/027) and by the FWO and F.R.S.-FNRS under the Excellence of Science (EOS) programme (EOS No. 40007553).

Conflicts of interest

All authors state that they have no conflicts of interest.

Data availability

The data that support the findings of this study are available on request from the corresponding author. The data are not publicly available due to privacy and ethical restrictions.

References

1. Vos T, Flaxman AD, Naghavi M, et al. Years lived with disability (YLDs) for 1160 sequelae of 289 diseases and injuries 1990-2010: a systematic analysis for the global burden of disease study 2010. *Lancet*. 2012;380(9859):2163–2196. https://doi.org/10.1016/S0140-6736(12)61729-2
2. Roberts BC, Thewlis D, Solomon LB, Mercer G, Reynolds KJ, Perilli E. Systematic mapping of the subchondral bone 3D microarchitecture in the human tibial plateau: variations with joint alignment. *J Orthop Res*. 2017;35(9):1927–1941. https://doi.org/10.1002/jor.23474
3. Rapagna S, Roberts BC, Solomon LB, Reynolds KJ, Thewlis D, Perilli E. Tibial cartilage, subchondral bone plate and trabecular bone microarchitecture in varus- and valgus-osteoarthritis versus controls. *J Orthop Res*. 2021;39(9):1988–1999. https://doi.org/10.1002/jor.24914
4. Chang J, Chen T, Yan Y, et al. Associations between the morphological parameters of proximal tibiofibular joint (PTFJ) and changes in tibiofemoral joint structures in patients with knee osteoarthritis. *Arthritis Res Ther*. 2022;24(1):1–9. https://doi.org/10.1186/s13075-022-02719-8
5. Ledingham J, Regan M, Jones A, Doherty M. Radiographic patterns and associations of knee osteoarthritis. *Ann Rheum Dis*. 1993;52:520–526.
6. Schipplein OD, Andriacchi TP. Interaction between active and passive knee stabilizers during level walking. *J Orthop Res*. 1991;9(1):113–119. https://doi.org/10.1002/jor.1100090114
7. Cerejo R, Dunlop DD, Cahue S, Channin D, Song J, Sharma L. The influence of alignment on risk of knee osteoarthritis progression according to baseline stage of disease. *Arthritis Rheum*. 2002;46(10):2632–2636. https://doi.org/10.1002/art.10530
8. Holzer LA, Kraiger M, Talakic E, et al. Microstructural analysis of subchondral bone in knee osteoarthritis. *Osteoporos Int*. 2020;31(10):2037–2045. https://doi.org/10.1007/s00198-020-05461-6
9. Roberts BC, Solomon LB, Mercer G, Reynolds KJ, Thewlis D, Perilli E. Relationships between in vivo dynamic knee joint loading, static alignment and tibial subchondral bone microarchitecture in end-stage knee osteoarthritis. *Osteoarthr Cartil*. 2018;26(4):547–556. https://doi.org/10.1016/j.joca.2018.01.014
10. Han X, Cui J, Xie K, et al. Association between knee alignment, osteoarthritis disease severity, and subchondral trabecular bone microarchitecture in patients with knee osteoarthritis: a cross-sectional study. *Arthritis Res Ther*. 2020;22(1):203–211. https://doi.org/10.1186/s13075-020-02274-0
11. Colyn W, Azari F, Bellemans J, van Lenthe GH, Scheys L. Microstructural adaptations of the subchondral bone are related to the mechanical axis deviation in end stage varus OA knees. *Eur Cells Mater*. 2023;45:60–71. https://doi.org/10.22203/eCM.v045a05
12. Beuf O, Ghosh S, Newitt DC, et al. Magnetic resonance imaging of normal and osteoarthritic trabecular bone structure in the human knee. *Arthritis Rheum*. 2002;46(2):385–393. https://doi.org/10.1002/art.10108
13. Lahm A, Dabravolski D, Rödig J, Esser J, Erggelet C, Kasch R. Varying development of femoral and tibial subchondral bone tissue and their interaction with articular cartilage during progressing osteoarthritis. *Arch Orthop Trauma Surg*. 2020;140(12):1919–1930. https://doi.org/10.1007/s00402-020-03480-w

14. Kellgren JH, Lawrence JS. Radiological assessment of osteo-arthrosis. *Ann Rheum Dis*. 1956;16(4):494–502. https://doi.org/10.1136/ard.16.4.494
15. Tassani S, Perilli E. On local micro-architecture analysis of trabecular bone in three dimensions. *Int Orthop*. 2013;37(8):1645–1646. https://doi.org/10.1007/s00264-013-1989-z
16. Harrigan TP, Jasty M, Mann RW, Harris WH. Limitations of the continuum assumption in cancellous bone. *J Biomech*. 1988;21(4):269–275. https://doi.org/10.1016/0021-9290(88)90257-6
17. Perilli E, Bala Y, Zebaze R, Reynolds KJ, Seeman E. Regional heterogeneity in the configuration of the intracortical canals of the femoral shaft. *Calcif Tissue Int*. 2015;97(4):327–335. https://doi.org/10.1007/s00223-015-0014-5
18. Bellemans J, Colyn W, Vandenneucker H, Victor J. The Chitranjan Ranawat award. *Clin Orthop Relat Res*. 2012;470(1):45–53. https://doi.org/10.1007/s11999-011-1936-5
19. Paley D, Pfeil J. Prinzipien der kniegelenknahen Deformitätenkorrektur. *Orthopade*. 2000;29(1):18–38. https://doi.org/10.1007/PL00003691
20. Lim BW, Hinman RS, Wrigley TV, Sharma L, Bennell KL. Does knee malalignment mediate the effects of quadriceps strengthening on knee adduction moment, pain, and function in medial knee osteoarthritis? A randomized controlled trial. *Arthritis Care Res*. 2008;59(7):943–951. https://doi.org/10.1002/art.23823
21. Adouni M, Shirazi-Adl A. Evaluation of knee joint muscle forces and tissue stresses-strains during gait in severe OA versus normal subjects. *J Orthop Res*. 2014;32(1):69–78. https://doi.org/10.1002/jor.22472
22. Kroker A, Zhu Y, Manske SL, Barber R, Mohtadi N, Boyd SK. Quantitative in vivo assessment of bone microarchitecture in the human knee using HR-pQCT. *Bone*. 2017;97:43–48. https://doi.org/10.1016/j.bone.2016.12.015
23. Bouxsein ML, Boyd SK, Christiansen BA, Guldberg RE, Jepsen KJ, Müller R. Guidelines for assessment of bone microstructure in rodents using micro-computed tomography. *J Bone Miner Res*. 2010;25(7):1468–1486. https://doi.org/10.1002/jbmr.141
24. Hildebrand T, Rüegsegger P. Quantification of bone microarchitecture with the structure model index. *Comput Methods Biomech Biomed Engin*. 1997;1(1):15–23. https://doi.org/10.1080/01495739708936692
25. Imhof H, Sulzbacher I, Grampp S, Czerny C, Youssefzadeh S, Kainberger F. Subchondral bone and cartilage disease: a rediscovered functional unit. *Investig Radiol*. 2000;35(10):581–588. https://doi.org/10.1097/00004424-200010000-00004
26. Sharma L, Song J, Felson DT, Cahue S, Shamiyeh E, Dunlop DD. The role of knee alignment in disease progression and functional decline in knee osteoarthritis. *JAMA*. 2001;286(2):188–195. https://doi.org/10.1001/jama.286.2.188